



# Initial evaluation of diaphragm seismic demand in a half-scale shake table test

D. Zhang<sup>1</sup>, R. B. Fleischman<sup>2</sup>, M. Mielke<sup>3</sup> & Z. Zhang<sup>2</sup>

<sup>1</sup>*School of Engineering, Nazarbayev University, Kazakhstan*

<sup>2</sup>*Department of Civil Engineering, University of Arizona, USA*

<sup>3</sup>*M3 Engineer, USA*

## Abstract

This paper presents an initial evaluation of the seismic demand for diaphragms during a shake table test of a three-story precast concrete structure. Each level of the test structure contained a different precast concrete floor construction technique: topped double tees on the lower level; topped hollow core on the middle floor; and pretopped double tees on the top floor. The diaphragms were designed and detailed according to a new design methodology developed as part of parallel research. The structure was subjected to a series of 16 strong ground motions with increasing intensity including design-basis and maximum considered earthquakes for which the diaphragms were designed. In the paper, the major diaphragm global and local response is quantified. Conclusions are drawn regarding the observed diaphragm behavior.

*Keywords: precast concrete; diaphragm, seismic response, shake table test.*

## 1 Introduction

A half-scale shake table test of a diaphragm-sensitive precast concrete structure was conducted at the Englekirk Structural Engineering Center of the University of California, San Diego (UCSD) [1] as part of a multi-university research project tasked with developing a new seismic design methodology for precast concrete floor diaphragms [2]. This paper presents quantitative results from the testing program focusing on the response of the diaphragms. The results presented in this paper serves as a reference for analytical model calibration efforts, occurring in parallel, as part of the development of diaphragm design



factors for codification of the new precast concrete diaphragm methodology. Conclusions are drawn regarding the observed diaphragm behavior.

## 2 Shake table tests

This section summarizes the design of the floor diaphragms for the shake table test. The reader is referred to [1] for a detailed description of the overall shake table testing program, including testing facility, specimen production, construction and details, testing sequence, peak responses and test observations. The design and test information presented in this section are in half-scale.

### 2.1 Test structure

The half-scale precast structure specimen is shown in the plan in Figure 1. Each level of the structure contained a different precast concrete floor construction technique (see Fig. 1(b)–(d)): topped double tees (DT) on the lower level; topped hollow core (HC) on the middle floor; and pretopped DT on the top floor. The structure aspect ratio in plan of 3.5 and lateral force resisting system layout [perimeter post-tension (PT) shear walls] are configured so as to create a diaphragm-critical structure in the direction of the shake table excitation (indicated in Fig. 1(d)).

The precast unit and diaphragm reinforcement layout for each floor is shown in Figure 1(b)–(d). As the structure is symmetric, each layout is indicated on a half-floor plan. The first half-floor plan (see Fig. 1(a)) shows the typical instrumentation layout.

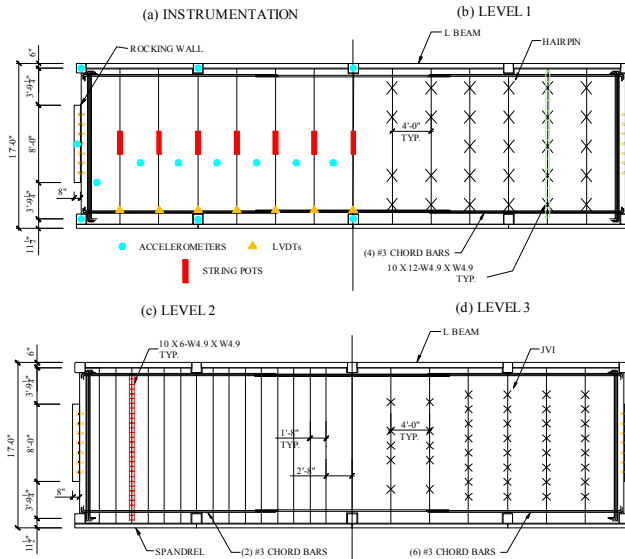


Figure 1: Shake table specimen.

## 2.2 Diaphragm design

The diaphragms of the test specimen were designed and detailed according to a new design methodology developed as part of the research [3]. In this design methodology, diaphragm design forces are aligned to diaphragm performance targets using three different design options. A reduced design option (RDO) was selected for the diaphragm design of the test structure with the following performance targets at maximum considered earthquake (MCE): (1) inelastic flexural response within the allowable diaphragm reinforcement deformation capacity; and (2) elastic shear response. To achieve these performance targets, the design methodology involves three primary modifications to current code: (1) an amplification factor ( $\Psi_R$ ) is applied to current diaphragm design forces, termed baseline design force; (2) a shear overstrength factor ( $\Omega_v$ ) is applied to the diaphragm shear design; and (3) high deformability elements (HDE) are used for the diaphragm reinforcement.

The diaphragm baseline design force was determined based on the current code equivalent lateral force (ELF) method used for the LFRS design. Although the LFRS of the test structure is the innovated PT wall which was designed using displacement based design method for Berkeley CA [4], this LFRS design is equivalent to a special shear wall ( $R=6$ ,  $\Omega_o=2.5$ ,  $C_d=5$ ) according to the current code [5]. The ELF calculation for the test specimen in half scale is shown in Table 1. The diaphragm force  $F_{px}$  (53.8 kips) at top floor is selected as the diaphragm baseline design force and applied to all the three floors according to the new design methodology.

Table 1: ELF calculation for the test specimen.

Story	$h_x$	$w_x$	$w_x h_x^k$	$c_{vx}$	$F_x$	$F_{px}$
	[ft]	[kips]			[kips]	[kips]
3	19.5	77.6	1513	0.49	53.8	<b>53.8</b>
2	13	82.1	1067	0.35	37.9	47.1
1	6.5	77.2	501	0.16	17.8	42.8
Summation		237	3082	1.00	109	

The diaphragm design factors for the test specimen were calibrated based on preliminary analytical studies. The final selected design factors are:  $\Psi_R = 1.34$  and  $\Omega_v = 1.61$ , which are closed to the values ( $\Psi_R = 1.35$  and  $\Omega_v = 1.53$ ) calculated from design equations proposed in [3] (BSSC TS4 2009). For the RDO design, the HDE reinforcement details for each floor diaphragm are used and shown in Figure 1(b)–(d) including: (1) dry chord connectors and JVI Vector connectors on the pretopped double tee 3rd floor; (2) continuous chord reinforcement and ductile welded-wire ladder reinforcement (WWR) at the panel joints for the topped non-composite 2nd floor hollow core diaphragm; and (3) continuous chord reinforcement, ductile ladder, and hairpin flange-to-flange connectors for the topped composite 1st floor double tee diaphragm.

The diaphragm designs for flexural critical (at diaphragm midspan) and shear critical joints (at diaphragm ends) are shown in Table 2. The diaphragm required design moment ( $M_u$ ) and shear ( $V_u$ ) are calculated using the simply supported horizontal beam method. The diaphragm nominal strength is determined at the joints. The design shear and tension strength values for individual diaphragm reinforcement elements (connectors or bars) are obtained from the test database of diaphragm connector properties [6]. The nominal shear strength ( $V_n$ ) is calculated the summation along the joint includes the chord reinforcement contribution to shear strength. The nominal moment strength ( $M_n$ ) is calculated as the moment at which the chord reinforcement reaches its tensile yield stress based on a strain compatibility procedure [3] that includes the contribution of the shear reinforcement to flexure. No reinforcing bar cut-off and only one spacing variation for JVI Vector and Hairpin connector are imposed along the diaphragm span (refer to Fig. 1(a)).

Table 2: Diaphragm joint design.

Story	$F_{px}$	$\Psi_R F_{px}$	$M_u$	$\phi M_n$	$V_n$	$\Omega_v$
	[kips]	[kips]	[k-ft]	[k-ft]	[kips]	
3	53.8	71.9	503	503	58	1.61
2	53.8	71.9	503	507	59	1.63
1	53.8	71.9	503	508	62	1.71

### 2.3 Instrumentation

The specimen was instrumented with five types of sensors (totaling 651) that measured accelerations, displacements or deformations, strains, and pressures. There were five different data acquisition systems (DAQ) with varying sampling rates that were post-processed to a common 240 samples per second. Accelerometers were placed throughout the specimen (on the diaphragm, the walls, the columns, etc.), mostly oriented in the direction of the shaking with some in the transverse and vertical directions. Four GPS antennas were used to monitor global displacement, while string potentiometers, linear voltage displacement transducers (LVDT), and linear potentiometers were used to measure relative displacements and deformations within the specimen. Strain gauges were placed on critical reinforcement bars such as the chords, the ductile WWR, and the energy-dissipation bars. They were also placed on the concrete at the toes of one wall to monitor compressive strains. Pressure transducers were used to measure the force in the post-tensioning tendons in the walls [1].

### 2.4 Test sequence

The test sequence is listed in Table 3. As seen, the specimen was subjected to a series of ground motions of increasing intensity. The series included 16 strong ground motions, including the design-basis and maximum considered earthquakes for the site (Berkeley CA) to which the diaphragms were designed.



To represent low, moderate, and high seismicity areas, Knoxville (KN), Seattle (SE), and Berkeley (BK) were chosen as the locations from which the ground motions would be taken (see Fig. 2 for design and earthquake response spectrum for each site)

Table 3: Test sequence.

#	Test ID	Site	Date	Intensity	Initial PT	Major event/failure
1	<b>KN-DBE 1</b>	<b>Knoxville</b>	<b>6-May-08</b>	<b>DBE</b>	<b>26%</b>	-
2	KN-DBE 2	Knoxville	6-May-08	DBE	26%	-
3	KN-DBE 3	Knoxville	7-May-08	DBE	26%	-
4	SE-DBE 1	Seattle	21-May-08	DBE	35%	Chord fracture at 3 <sup>rd</sup> floor midspan
5	SE-DBE 2	Seattle	12-Jun-08	DBE	35%	
6	SE-DBE 3	Seattle	12-Jun-08	DBE	35%	Chord fracture at 3 <sup>rd</sup> floor midspan & buckling at 2 <sup>nd</sup> floor midspan
7	SE-DBE 4	Seattle	20-Jun-08	DBE	35%	-
8	<b>BK-DBE 1</b>	<b>Berkeley</b>	<b>20-Jun-08</b>	<b>DBE</b>	<b>35%</b>	<b>PT strand failure initiation</b>
9	BK-MCE 1	Berkeley	20-Jun-08	MCE	35%	PT full tendon failure in the wall resulting in fracture of gravity system connections
10	BK-EDB 1	Berkeley	14-Jul-08	60% DBE	50%	Wall connection failure at 3 <sup>rd</sup> floor
11	BK-EDB 2	Berkeley	16-Jul-08	60% DBE	50%	-
12	<b>BK-EMC 1</b>	<b>Berkeley</b>	<b>16-Jul-08</b>	<b>DBE</b>	<b>50%</b>	<b>Crack in DT at 3<sup>rd</sup> floor wall connection</b>
13	BK-EMC 2	Berkeley	17-Jul-08	DBE	50%	Failure of sliders @ outrigger
14	BK-EDB 3	Berkeley	22-Jul-08	DBE	50%	Wall connection failure at 2nd floor
15	BK-EMC 3	Berkeley	23-Jul-08	DBE	50%	Failure of sliders @ outrigger
16	BK-MCE *	Berkeley	28-Jul-08	MCE	50%	Floor unseating leading to partial collapse of 3 <sup>rd</sup> floor

Indicates successful test.



Among these 16 tests with strong ground motions, nine tests were considered as successful tests without major structure damages or failures. This paper will primarily present four test (see bold rows in Table 4) results from these nine tests for each ground motion intensity level including: (1) Test 1: KN DBE 1 representing KN DBE; (2) Test 7: SE DBE 4 representing SE DBE; (3) Test 8: BK DBE 1 representing BK DBE; and (4) Test 12: BK EMC 1 representing BK MCE. The 5% response spectrum for the four ground motions is shown in Fig. 2.

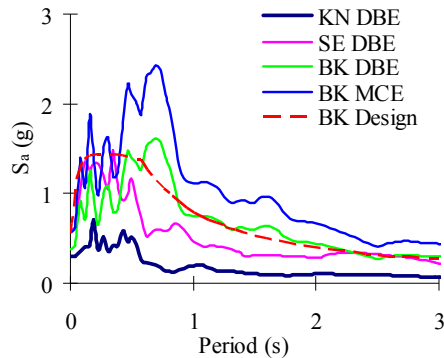


Figure 2: 5% response spectrum of ground motions.

### 3 Test results

In this section, the diaphragm global and local response is presented. Though the test was conducted at half scale, the response shown in this section is transformed into full scale.

Figure 3 shows the inertial force time histories of four different ground motion intensities in their entirety. The force is normalized by the design force  $\Psi_{RF_{px}}$  shown in Tables 2 and 3. The bracketed section in each plot indicates the time of major ground motion shaking and will be the focus of all time histories hereafter.

Figure 4 shows the normalized inertial force time histories of four different ground motion intensities in the major shaking period (see Fig. 3). As seen, except for the low level earthquake: KN DBE (see Fig. 4(a)), the force demand in the diaphragm all exceeded the design strength (see Fig. 4(b)–(d)), which indicates the yielding of diaphragm during the earthquakes. The yielding of diaphragm is expected since the diaphragm is designed for RDO which allows inelastic response in both design basis and maximum considered earthquakes. The exceedance of the design force during the earthquake is caused by the strain hardening of the diaphragm reinforcement.

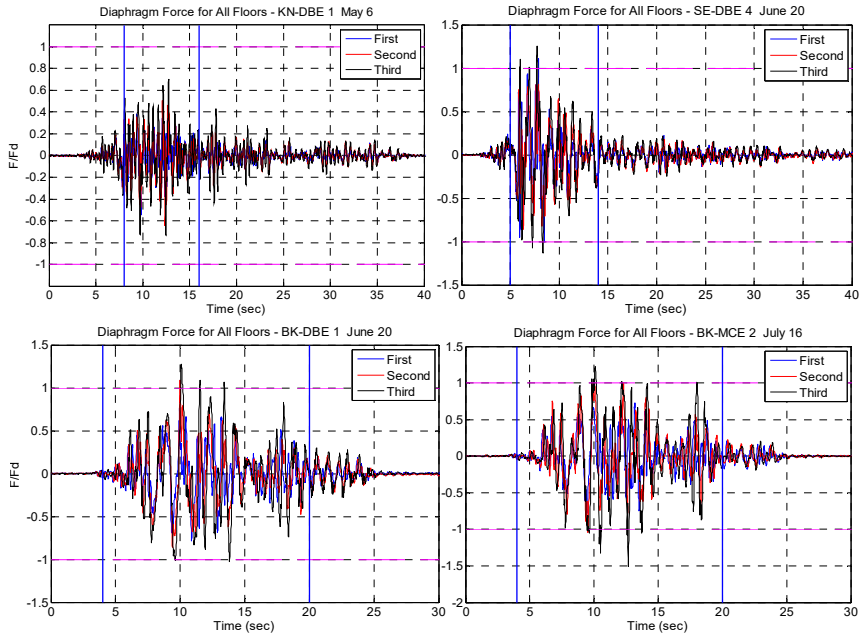


Figure 3: Diaphragm inertial force response, full history: (a) KN; (b) SE; (c) BK-DB; (d) BK-MC.

Figure 5 shows the midspan deformation time histories of four different ground motion intensities in the major shaking period (see Fig. 3). As seen, the maximum diaphragm deformation occurs at the top floor. The diaphragm deformation response for the three floors is not always in phase and sometimes is completely out-of-phase. This out-of-phase response is originated from the structural higher dynamic modes.

Figure 6 shows the diaphragm hysteresis response: normalized diaphragm forces vs. diaphragm midspan deformation for four different ground motion intensities. The diaphragm exhibits good ductility as the diaphragm strength does not degrade under large inelastic deformation demand. Also noticed, the diaphragm stiffness degrades with the yielding of the diaphragm especially for the 2<sup>nd</sup> and 3<sup>rd</sup> floor.

Figure 7 shows the inter-story drift time histories of four different ground motion intensities in the major shaking period (see Fig. 3). As seen, the inter-story drift demand is amplified by the deformation of the diaphragm especially when the diaphragm yields. However, the maximum inter-story drift demand is still less than the current code requirement of 2% [5].

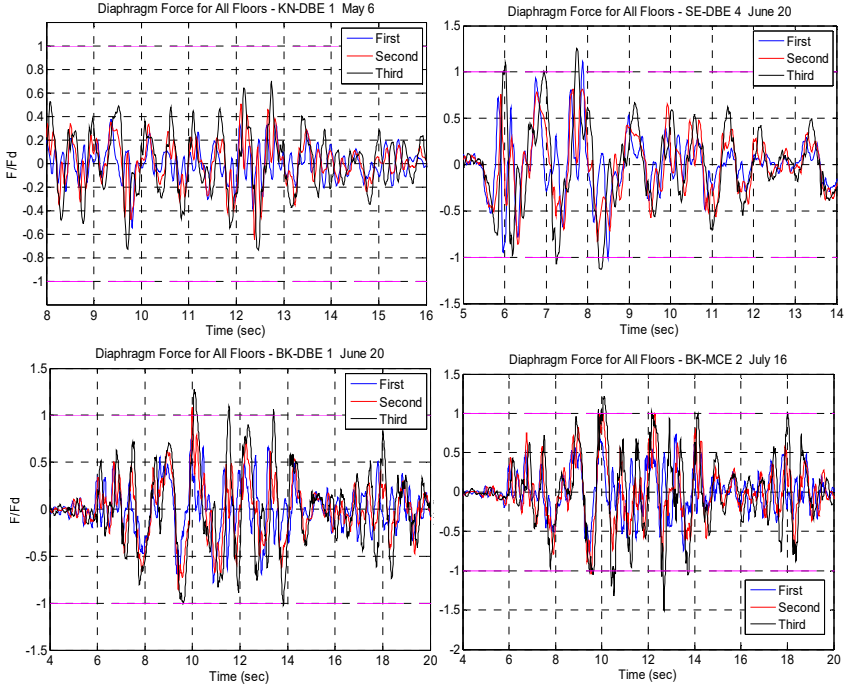


Figure 4: Diaphragm inertial force: (a) KN; (b) SE; (c) BK-DB; (d) BK-MC.

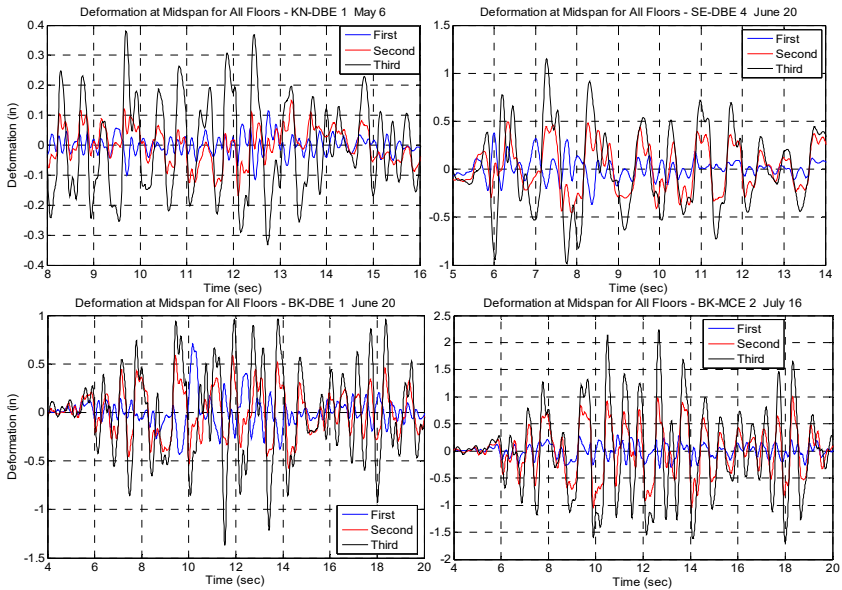


Figure 5: Diaphragm deformation: (a) KN; (b) SE; (c) BK-DB; (d) BK-MC.



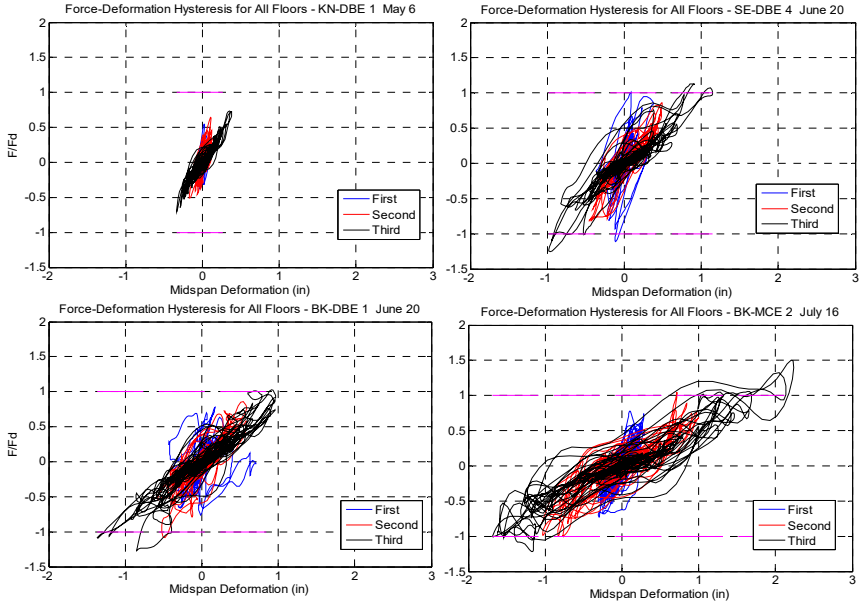


Figure 6: Diaphragm hysteresis: (a) KN; (b) SE; (c) BK-DB; (d) BK-MC.

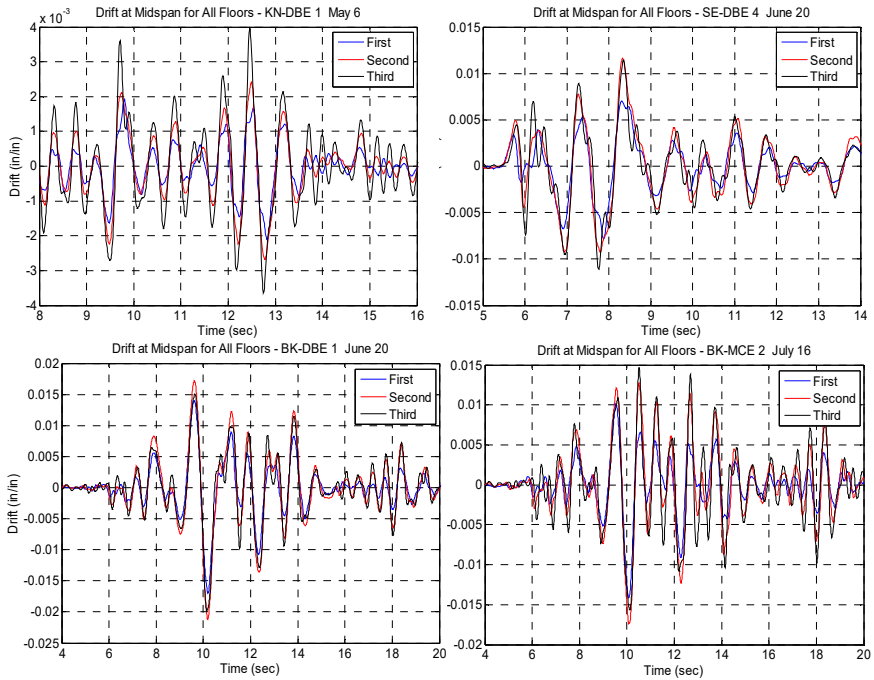


Figure 7: Diaphragm interstory drift: (a) KN; (b) SE; (c) BK-DB; (d) BK-MC.



Figure 8 shows the diaphragm midspan joint opening time histories of four different ground motion intensities in the major shaking period (see Fig. 3). The diaphragm joint opening is normalized by the yielding deformation of the diaphragm reinforcement. As seen, the diaphragm joint opening exceeds the yield deformation in all the earthquakes except for the low level earthquake: KN DBE. However, the maximum inelastic demand in the joint is less than the ductility capacity of HDE which is found as 10.0 in the diaphragm reinforcement test [6].

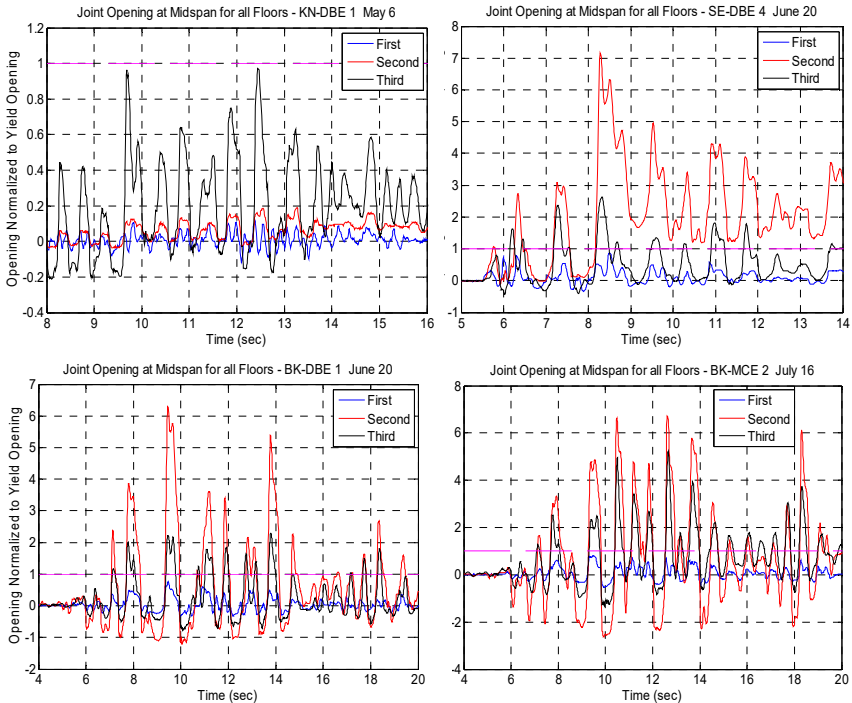


Figure 8: Diaphragm joint opening: (a) KN; (b) SE; (c) BK-DB; (d) BK-MC.

## 4 Conclusions

The half-scale shake table test program of a diaphragm-sensitive precast concrete structure was conducted at NEES shake table at the Englekirk Structural Engineering Center of the UCSD. The RDO design proposed in the new diaphragm seismic design methodology is used for diaphragm design of the three-story precast concrete test structure. The test structure was successively subjected to 16 strong ground motions including design-basis and maximum considered earthquakes for which the diaphragms were designed. The following conclusions are made for the diaphragm seismic response:

- (1) The diaphragm yielded in flexure as expected for the RDO design. The inelastic opening demand in diaphragm reinforcement under MCE was within the allowable deformation of HD elements which indicates that the proposed diaphragm force amplification factor ( $\Psi_R$ ) is sufficient.
- (2) The inter-story drift is within the design limit (2%) even though it is amplified by the diaphragm inelastic deformation.
- (3) The top floor typically has largest diaphragm force and deformation demand.
- (4) The diaphragm response for different floors is not always in phase due to higher dynamic modes.
- (5) The diaphragm designed with RDO shows good ductility though significant inelastic response is observed during the earthquakes.
- (6) The diaphragm stiffness degrades with the increase of the diaphragm inelastic deformation response.

## Acknowledgements

This research was supported by the Precast/Prestressed Concrete Institute (PCI), the Charles Pankow Foundation, and the National Science Foundation (NSF) under Grant CMS-0324522 and SGER Supplement CMMI-0623952. The authors are grateful for this support. Any opinions, findings, and conclusions or recommendations expressed in this material are those of the author(s) and do not necessarily reflect the views of the National Science Foundation.

## References

- [1] Schoettler M.J., Belleri A., Zhang D., Restrepo J. Fleischman R.B. (2009). Preliminary Results of the Shake-table Testing for Development of A Diaphragm Seismic Design Methodology. *PCI Journal*; 54 (1): 100-124.
- [2] Fleischman R.B., Restrepo J.I, Naito C.J., Sause R., Zhang D. and Schoettler M. (2013). Integrated Analytical and Experimental Research to Develop a New Seismic Design Methodology for Precast Concrete Diaphragms. Special Issue of the ASCE Journal of Structural Engineering on NEES: Advances in Earthquake Engineering; V139 (7).
- [3] Building Seismic Safety Council, Committee TS-4. (2009). Seismic Design Methodology for Precast Concrete Floor Diaphragms. Part III, NEHRP Recommended Seismic Provisions, Federal Emergency Management Agency, Washington, D.C.
- [4] Belleri, A., Schoettler, M. J., Restrepo, J. I., and Fleischman, R. B. (2014). Dynamic Behavior of Rocking and Hybrid Cantilever Walls in a Precast Concrete Building (with Appendix). *ACI Structural Journal*, 111(3).
- [5] ASCE 7-05. (2005). Minimum Design Loads for Buildings and Other Structures. American Society of Civil Engineering.
- [6] Naito, C. and Ren, R. (2008). Development of a Seismic Design Methodology for Precast Diaphragms – Phase 1C Summary Report, ATLSS Report No. 08-09, ATLSS Center, Lehigh University.

